The Generalized Method of Characteristics for Waveform Relaxation Analysis of Lossy Coupled Transmission Lines

FUNG-YUEL CHANG, SENIOR MEMBER, IEEE

Abstract — **The transient response of lossy coupled transmission lines is simulated by iterative waveform relaxation analyses of equivalent disjoint networks constructed with congruence transformers, FFT waveform generators, and characteristic impedances synthesized by the Padé approximation. A phenomenal two order reduction of CPU time and one order savings in computer memory have been achieved. A lossy directional coupler is simulated for illustration.**

I. Introduction

THE METHOD OF CHARACTERISTICS (MC) and the method of waveform relaxation (WR) are two seemingly unrelated computational algorithms being developed to improve efficiency in the computer-aided analysis of large-scale electrical circuits. The MC [1] is a technique for solving partial differential equations (PDE's) by transformation of PDE's into ordinary differential equations (ODE's) along the characteristic directions, whereas the WR method [2] is a technique for solving systems of ODE's by iteration and system decomposition. The MC was introduced by Branin [3] for the transient analysis of an ideal transmission line. His idea was subsequently generalized [4] and implemented in circuit simulators for the analysis of coupled transmission lines. Since the MC was conceived for the solution of PDE's [5], other CAD applications of the algorithm have also been specialized for the discrete-time simulation of distributed parameter networks [6]–[8]. At the other extreme of development of CAD tools, the WR method was tailored for the waveform simulation of lumped-parameter systems, of which the MOS integrated circuits (IC's) have received most of the attention [2], [9], [10].

It is the purpose of this paper to show that by generalizing the method of characteristics for waveform relaxation analysis, time-domain simulations of lumped-parameter networks interconnected with coupled transmission lines can be carried out more efficiently. The generalized method of characteristics (GMC) has been implemented in ICD [11] on an experimental basis. In comparison to the classical discrete-time simulation, a phenomenal two order reduction in computer simulation time and one order savings in computer memory requirements have been achieved by applying the GMC.

In this, one of a sequence of papers devoted to the waveform relaxation analysis of distributed-parameter networks, we focus our attention on an n-conductor lossy shielded stripline system which is surrounded by a homogeneous, leakage-free dielectric medium. The organization of this paper is outlined as follows. It is shown in Section II that insofar as the terminal characteristic is concerned, the lossy stripline system is equivalent to a set of decoupled lossy transmission lines interconnected with congruence transformers. From the equivalent circuit, canonical expressions for the terminal voltages are derived and expanded into infinite series leading to the sequence of incident and reflected waves for the time-domain characterization of the stripline system. In Section III, the classical MC is extended for deriving the equivalent 2-port network of a lossy transmission line. Each port of the 2-port network is constructed with a lossy characteristic impedance connected in series with a voltage source attenuated by the exponential propagation function of the lossy transmission line. The lossy characteristic impedance is synthesized by applying the Padé approximation, and the exponential propagation function is simulated by the fast Fourier transform (FFT). In Section IV, the classical MC is generalized for waveform relaxation analysis. An iteration scheme for generating the sequence of incident and reflected waves using a circuit simulator is established. In Section V, a three-conductor lossy directional coupler driven by a bipolar emitter coupled logic gate (ECL) is simulated to illustrate the advantage of the waveform relaxation analysis over the classical discrete-time simulation. Concluding remarks are contained in Section VI, along with a description of the ongoing research work on the generalized method of characteristics.

II. Decoupled Equivalent Circuits and Wave Propagation in a Lossy Stripline System

Consider an array of n parallel lossy conductors embedded in a homogeneous, leakage-free dielectric medium. Wave propagation in such a lossy stripline system is de-

Manuscript received March 29, 1989; revised July 14, 1989.

The author is with the General Technology Division, International Business Machines Corporation, East Fishkill Facility, Hopewell Junction, NY 12533.

IEEE Log Number 8930955.

scribed by the generalized telegraphist's equation

$$\frac{\partial \boldsymbol{v}(x,t)}{\partial x} = -\boldsymbol{L}\frac{\partial \boldsymbol{i}(x,t)}{\partial t} - \boldsymbol{R}\boldsymbol{i}(x,t) \tag{1a}$$

$$\frac{\partial \boldsymbol{i}(x,t)}{\partial x} = -\boldsymbol{C}\frac{\partial \boldsymbol{v}(x,t)}{\partial t}, \qquad 0 \leqslant x \leqslant l \tag{1b}$$

where[1] $\boldsymbol{v}(x,t)$ and $\boldsymbol{i}(x,t)$ are column vectors defining the voltages $v_k(x,t)$ and currents $i_k(x,t)$ on the conductors $k=1,2\cdots n$. $\boldsymbol{R}$ is the diagonal matrix of the per-unit-length (PUL) resistance of the conductors. $\boldsymbol{L}$ and $\boldsymbol{C}$ are the n by n symmetric matrices of the PUL inductance and capacitance, and

$$\boldsymbol{LC} = (1/v^2)\boldsymbol{I}_n \tag{2}$$

where v is the wave propagation velocity and $\boldsymbol{I}_n$ is the nth-order identity matrix.

Since both $\boldsymbol{L}$ and $\boldsymbol{R}^{-1/2} = \operatorname{diag}(1/\sqrt{R_k})$ are real, symmetric, and positive-definite, the same is true of the time-constant matrix

$$\boldsymbol{T} = \boldsymbol{R}^{-1/2}\boldsymbol{L}\boldsymbol{R}^{-1/2} = \boldsymbol{W}\operatorname{diag}(\tau_k)\boldsymbol{W}^{-1}, \qquad \boldsymbol{W}^{-1} = \boldsymbol{W}^t \tag{3}$$

which can always be diagonalized with positive eigenvalues $\{\tau_k\}$ $(k=1,2,3\cdots n)$. By defining the congruence transformer matrix [4]

$$\boldsymbol{X} = \boldsymbol{R}^{1/2}\boldsymbol{W}\operatorname{diag}\left(\sqrt{\tau_k/L_k}\right) \tag{4}$$

and applying the linear transformation

$$\boldsymbol{v}(x,t) = \boldsymbol{X}\boldsymbol{e}(x,t) \qquad \boldsymbol{i}(x,t) = (\boldsymbol{X}^t)^{-1}\boldsymbol{j}(x,t) \tag{5}$$

to (1) and using (2) and (3), we obtain

$$\frac{\partial \boldsymbol{e}(x,t)}{\partial x} = -\tilde{\boldsymbol{L}}\frac{\partial \boldsymbol{j}(x,t)}{\partial t} - \tilde{\boldsymbol{R}}\boldsymbol{j}(x,t) \tag{6a}$$

$$\frac{\partial \boldsymbol{j}(x,t)}{\partial x} = -\tilde{\boldsymbol{C}}\frac{\partial \boldsymbol{e}(x,t)}{\partial t} \qquad (0 \leqslant x \leqslant l). \tag{6b}$$

Here

$$\tilde{\boldsymbol{R}} = \operatorname{diag}(L_k/\tau_k) \qquad \tilde{\boldsymbol{L}} = \operatorname{diag}(L_k)$$

$$\tilde{\boldsymbol{C}} = \operatorname{diag}(1/v^2 L_k) \tag{7}$$

are all diagonal matrices, $\{L_k\}$ $(k=1,2\cdots n)$ are the arbitrary positive constants preassigned in (4), and $\{\tau_k\}$ are the set of eigenvalues defined in (3). Equation (6) describes a set of n decoupled transmission lines. Thus, as far as the terminal characteristics are concerned, the lossy stripline system is equivalent to a set of n decoupled lossy transmission lines connected with congruence transformers as shown in Fig. 1. From the decoupled equivalent circuit we can relate the input and output of the lossy stripline

[1]Symbols in boldface italics designate matrices and vectors. The superscripts -1 and t denote matrix inversion and matrix transposition, respectively. The diagonal matrix $\operatorname{diag}(a_1, a_2, \cdots, a_n)$ is abbreviated as $\operatorname{diag}(a_k)$. $[\boldsymbol{A}]_{i,j}$ designates the (i,j)th element of the $\boldsymbol{A}$ matrix.

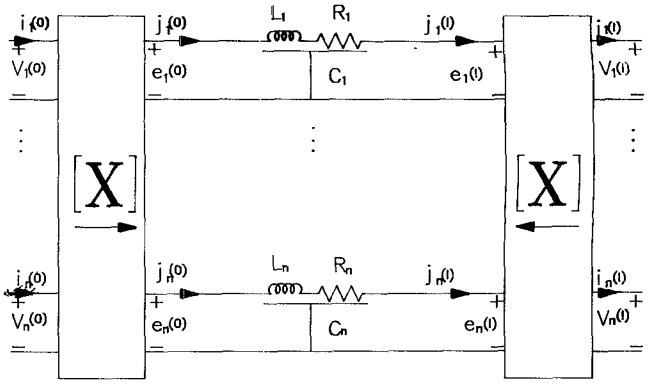

Fig. 1. The decoupled equivalent circuit of an n-conductor lossy coupled transmission-line system.

system by the following chain-matrix formulation[2]:

$$\begin{bmatrix} \boldsymbol{V}(0) \\ \boldsymbol{I}(0) \end{bmatrix} = \begin{bmatrix} \boldsymbol{X} & 0 \\ 0 & (\boldsymbol{X}^t)^{-1} \end{bmatrix} \cdot \begin{bmatrix} \operatorname{diag}(\cosh\theta_k) & \operatorname{diag}(Z_{0k}\sinh\theta_k) \\ \operatorname{diag}[(1/Z_{0k})\sinh\theta_k] & \operatorname{diag}(\cosh\theta_k) \end{bmatrix} \begin{bmatrix} \boldsymbol{X}^{-1} & 0 \\ 0 & \boldsymbol{X}^t \end{bmatrix} \begin{bmatrix} \boldsymbol{V}(l) \\ \boldsymbol{I}(l) \end{bmatrix} \tag{8a}$$

where the propagation functions $\{\theta_k\}$ and the characteristic impedance $\{Z_{0k}\}$ are defined in terms of the decoupled transmission-line parameters:

$$\theta_k = \sqrt{sC_k(R_k + sL_k)}\, l \tag{8b}$$

$$Z_{0k} = \sqrt{(R_k + sL_k)/sC_k}\,. \tag{8c}$$

The chain-matrix formulation allows the transmission-line terminal voltages to be expressed in explicit forms. To simplify the derivation, (8a) is transformed into the following equivalent forms:

$$\boldsymbol{V}(0) - \boldsymbol{Z}_0\boldsymbol{I}(0) = \boldsymbol{\Phi}[\boldsymbol{V}(l) - \boldsymbol{Z}_0\boldsymbol{I}(l)] \tag{9a}$$

$$\boldsymbol{V}(l) + \boldsymbol{Z}_0\boldsymbol{I}(l) = \boldsymbol{\Phi}[\boldsymbol{V}(0) + \boldsymbol{Z}_0\boldsymbol{I}(0)] \tag{9b}$$

where

$$\boldsymbol{Z}_0 = \boldsymbol{X}\operatorname{diag}(Z_{0k})\boldsymbol{X}^t \tag{9c}$$

$$\boldsymbol{\Phi} = \boldsymbol{X}\operatorname{diag}[\exp(-\theta_k)]\boldsymbol{X}^{-1} \tag{9d}$$

are the characteristic impedance matrix and the exponential propagation matrix of the lossy stripline system, respectively. We assume that the stripline system is terminated in Thevenin equivalent voltage sources $\{\boldsymbol{E}_A, \boldsymbol{E}_B\}$ and impedances $\{\boldsymbol{Z}_A, \boldsymbol{Z}_B\}$ as shown in Fig. 2. Thus substituting the boundary conditions

$$\boldsymbol{V}(0) = \boldsymbol{E}_A - \boldsymbol{Z}_A\boldsymbol{I}(0) \qquad \boldsymbol{V}(l) = \boldsymbol{E}_B + \boldsymbol{Z}_B\boldsymbol{I}(l)$$

into (9) for eliminating $\boldsymbol{I}(0)$ and $\boldsymbol{I}(l)$, we obtain

$$\begin{bmatrix} \boldsymbol{I}_n + \boldsymbol{Z}_0\boldsymbol{Z}_A^{-1} & -\boldsymbol{\Phi}(\boldsymbol{I}_n - \boldsymbol{Z}_0\boldsymbol{Z}_B^{-1}) \\ -\boldsymbol{\Phi}(\boldsymbol{I}_n - \boldsymbol{Z}_0\boldsymbol{Z}_A^{-1}) & \boldsymbol{I}_n + \boldsymbol{Z}_0\boldsymbol{Z}_B^{-1} \end{bmatrix} \begin{bmatrix} \boldsymbol{V}(0) \\ \boldsymbol{V}(l) \end{bmatrix} = \begin{bmatrix} \boldsymbol{Z}_0\boldsymbol{Z}_A^{-1} & \boldsymbol{\Phi}\boldsymbol{Z}_0\boldsymbol{Z}_B^{-1} \\ \boldsymbol{\Phi}\boldsymbol{Z}_0\boldsymbol{Z}_A & \boldsymbol{Z}_0\boldsymbol{Z}_B^{-1} \end{bmatrix} \begin{bmatrix} \boldsymbol{E}_A \\ \boldsymbol{E}_B \end{bmatrix}. \tag{10}$$

[2]Frequency- and time-domain functions are assigned by uppercase and lowercase letters, respectively, such as $\{\boldsymbol{V}, \boldsymbol{I}\}$ and $\{\boldsymbol{v}, \boldsymbol{i}\}$.

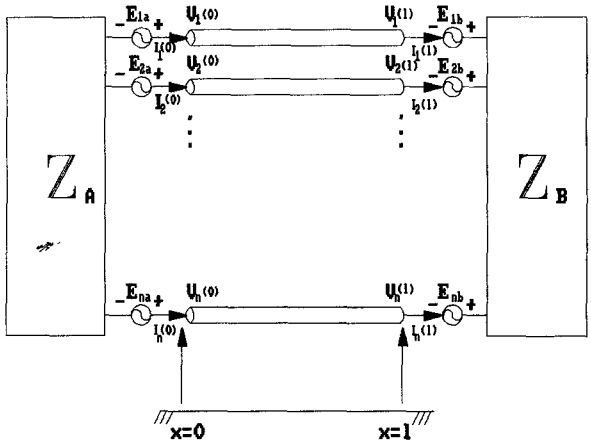

Fig. 2. An n-conductor system terminating in Thevenin's equivalent circuit.

Solving (10) using the inversion formula[3]

$$\begin{bmatrix} A & B \\ C & D \end{bmatrix}^{-1} =$$

$$\cdot \begin{bmatrix} \left(I_n - A^{-1}BD^{-1}C\right)^{-1}A^{-1} & 0 \\ 0 & \left(I_n - D^{-1}CA^{-1}B\right)^{-1}D^{-1} \end{bmatrix}$$

$$\cdot \begin{bmatrix} I_n & -BD^{-1} \\ -CA^{-1} & I_n \end{bmatrix}$$

yields the canonical expressions of the transmission-line terminal voltages

$$V(0) = (I_n - P)^{-1}U_A \tag{11a}$$

$$V(l) = (I_n - Q)^{-1}U_B \tag{11b}$$

where the propagation matrices

$$P = (I_n + \rho_A)\Phi\rho_B\Phi\rho_A(I_n + \rho_A)^{-1} \tag{12a}$$

$$Q = (I_n + \rho_B)\Phi\rho_A\Phi\rho_B(I_n + \rho_B)^{-1} \tag{12b}$$

simulate delay and attenuation of waveforms propagating in the stripline system. The equivalent voltage sources

$$U_A = (1/2)\left[(I_n + P\rho_A^{-1})(I_n - \rho_A)E_A + (I_n + \rho_A)\Phi(I_n - \rho_B)E_B\right] \tag{13a}$$

$$U_B = (1/2)\left[(I_n + \rho_B)\Phi(I_n - \rho_A)E_A + (I_n + Q\rho_B^{-1})(I_n - \rho_B)E_B\right] \tag{13b}$$

are functions of the reflection matrices:

$$\rho_A = (Z_A - Z_0)(Z_A + Z_0)^{-1} \tag{14a}$$

$$\rho_B = (Z_B - Z_0)(Z_B + Z_0)^{-1} \tag{14b}$$

Thus, by expanding the canonical expression (11) into

[3] A, B, C, D are $n \times n$ matrices and A, D are nonsingular. The inversion formula can be rearranged into many equivalent forms; however, only the present form leads to the canonical expression (11).

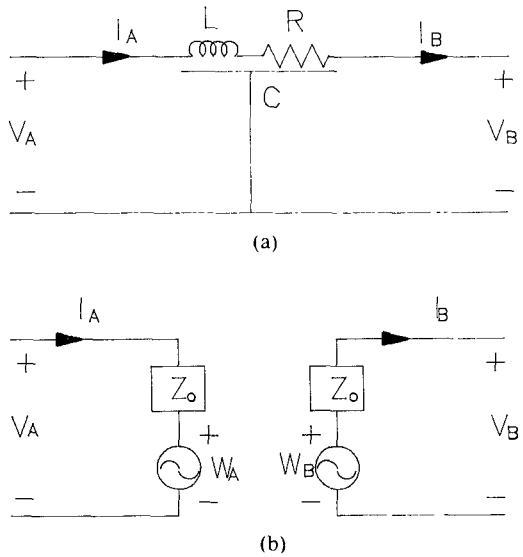

Fig. 3. (a) An RLC transmission line and (b) its equivalent disjoint 2-port network.

infinite (geometric progressive) series:

$$V(0) = U_A + PU_A + P^2U_A + P^3U_A + \cdots \tag{15a}$$

$$V(l) = U_B + QU_B + Q^2U_B + Q^3U_B + \cdots \tag{15b}$$

we observe that the transmission-line terminal voltages are composed of incident and reflected waves traveling back and forth on the conductors. The stripline terminal voltage waveforms can be derived by taking the inverse Laplace transform of (15), term by term. Such an analytic approach to the transient analysis of coupled lossy transmission lines is tedious and impractical. Instead, an iteration scheme for generating the sequence of incident and reflection waves using a circuit simulator will be described in Section IV. The equivalent disjoint network structure for generating the iterative waveforms will be described in the next section.

III. Padé Synthesis and FFT Simulation of a Lossy Transmission Line

In this section the classical MC is extended to include the conductor loss of a transmission line. For a single lossy transmission line, (9) degenerates to the following simple form:

$$V_A - Z_0I_A = [\exp(-\theta)](V_B - Z_0I_B) \tag{16a}$$

$$V_B + Z_0I_B = [\exp(-\theta)](V_A + Z_0I_A) \tag{16b}$$

where (V_A, I_A) and (V_B, I_B) are the terminal voltages and currents at the near end and the far end of the transmission line, as shown in Fig. 3(a). The expressions for the propagation constant and the characteristic impedance given in (8) are repeated here with the subscript k deleted for the simplicity of notation:

$$\theta(s) = \sqrt{sC(R + sL)}\,l \tag{16c}$$

$$Z_0 = \sqrt{(R + sL)/sC}\,. \tag{16d}$$

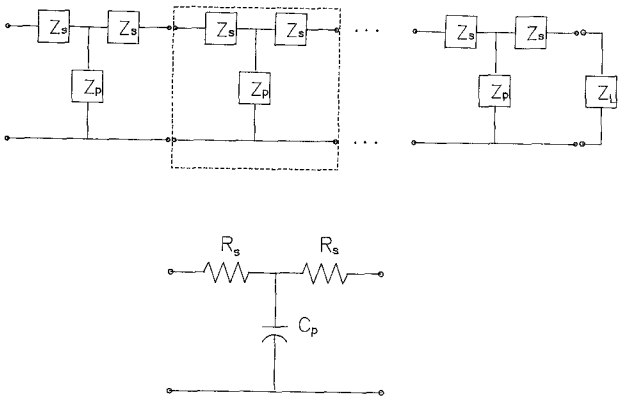

Fig. 4. A periodic ladder network constructed with symmetrical T net works.

By defining

$$W_A = [\exp(-\theta)](V_B - Z_0 I_B) \tag{17a}$$

$$W_B = [\exp(-\theta)](V_A + Z_0 I_A) \tag{17b}$$

(16a) and (16b) can be rewritten as follows:

$$V_A = Z_0 I_A + W_A \tag{18a}$$

$$V_B = -Z_0 I_B + W_B. \tag{18b}$$

Thus a lossy transmission line is equivalent to the disjoint 2-port network shown in Fig. 3(b). Eliminating I_B from (17a) using (18b) and eliminating I_A from (17b) using (18a), we obtain

$$W_A = [\exp(-\theta)](2V_B - W_B) \tag{19a}$$

$$W_B = [\exp(-\theta)](2V_A - W_A). \tag{19b}$$

Transient analysis of a lossy stripline system can be carried out by replacing each of the decoupled lossy line of Fig. 1 by the disjoint 2-port network of Fig. 3(b). Padé synthesis of the lossy characteristic impedance Z_0 and the simulation of W_A and W_B using FFT are described in the following subsections.

A. Padé Synthesis of the Lossy Characteristic Impedance $Z_0 = \sqrt{(R + sL)/sC}$

The characteristic impedance Z_0 of an *RLC* transmission line can be synthesized by the driving-point impedance of a ladder network constructed by using an infinite number of symmetrical T-network sections connected in tandem as shown in Fig. 4. To estimate the truncation error of using finite k sections for the lumped approximation of Z_0, the driving-point impedance of the ladder network terminating in short circuit, open circuit, and impedance Z_S are derived from the chain-matrix formulation, yielding the result

$$\underline{Z}^{(k)} = Z_0(Q_0^{2k} - 1)/(Q_0^{2k} + 1), \qquad Z^{(0)} = 0 \tag{20a}$$

$$\overline{Z}^{(k)} = Z_0(Q_0^{2k} + 1)/(Q_0^{2k} - 1), \qquad Z^{(0)} \to \infty \tag{20b}$$

$$Z^{(k)} = Z_0(Q_0^{2k+1} - 1)/(Q_0^{2k+1} + 1), \qquad Z^{(0)} = Z_S \tag{20c}$$

where

$$Z_0(s) = \sqrt{Z_S(Z_S + 2Z_P)} \tag{21a}$$

$$Q_0(s) = 1 + (Z_S/Z_P) + \sqrt{[2 + (Z_S/Z_P)](Z_S/Z_P)}. \tag{21b}$$

The series and shunt impedances Z_S and Z_P of the T network:

$$Z_S = R_s = \sqrt{L/C} \tag{22a}$$

$$Z_P = 1/sC_p, \qquad C_p = (2R_s/R)C = 2\sqrt{LC}/R \tag{22b}$$

are obtained by identifying (21a) with (16d). From (20) we observe that the characteristic impedance Z_0 is the geometric mean of $\underline{Z}^{(k)}$ and $\overline{Z}^{(k)}$: $Z_0 = \sqrt{\underline{Z}^{(k)}\overline{Z}^{(k)}}$ and is bounded below and above by $\underline{Z}^{(k)}$ and $\overline{Z}^{(k)}$:

$$Z_0 > \underline{Z}^{(k)} = Z_0 - 2Z_0/(Q_0^{2k} + 1)$$

$$Z_0 < \overline{Z}^{(k)} = Z_0 + 2Z_0/(Q_0^{2k} - 1).$$

To investigate the nature of approximating Z_0 by $Z^{(k)}$, we apply the transformations

$$z = R/sL \qquad y = \sqrt{z + 1} \tag{23}$$

and substitute (22) into (21) and convert (20c) into the following expression:

$$Z^{(k)}(y) = Z_0(y) - (y-1)^{2k+1}(2\sqrt{L/C}\,y) \Big/ [(y+1)^{2k+1} + (y-1)^{2k+1}].$$

Thus by virtue of the factor $(y-1)^{2k+1}$, whose first $2k$ derivatives vanish at $z = 0$, we obtain

$$\left.\frac{d^n Z^{(k)}(z)}{dz^n}\right|_{z=0} = \left.\frac{d^n Z_0(z)}{dz^n}\right|_{z=0} \qquad (n = 0,1,2,\cdots,2k).$$

Therefore the power series

$$Z^{(k)}(z) = \sum_{n=0}^{\infty} \left.\frac{d^n Z^{(k)}(z)}{dz^n}\right|_{z=0} \left(\frac{1}{n!}\right) z^n$$

$$Z_0(z) = \sum_{n=0}^{\infty} \left.\frac{d^n Z_0(z)}{dz^n}\right|_{z=0} \left(\frac{1}{n!}\right) z^n$$

are identical in the first $(2k+1)$ terms. A rational function

$$F_{m,n}(z) = \frac{P_m(z)}{Q_n(z)} = \frac{a_0 + a_1 z + a_2 z^2 + a_3 z^3 + \cdots + a_m z^m}{1 + b_1 z + b_2 z^2 + b_3 z^3 + \cdots + b_n z^n}$$

is said to be the Padé (m, n)th approximation of $F(z)$ [12] if the polynomials $P_m(z)$ and $Q_n(z)$ are so chosen that the coefficients in the power-series expansion of $F_{m,n}(z)$ agree with those of $F(z)$ from the constant term up to and including the z^{m+n} term. Thus we have proved that $Z^{(k)}(z)$ is the Padé (k, k) approximation of $Z_0(z)$.

B. The FFT Simulation of the Exponential Propagation Function

Although the exponential propagation function (16c) of a lossy transmission line can be synthesized as the voltage transfer function of either a ladder network or a symmetrical lattice network [13], we will not discuss the subject here. Instead, we will take advantage of the extreme efficiency of the FFT for deriving the waveforms of the voltage generators:

$$w_a(t) = F^{-1}\{\exp(-\theta)F[2v_b(t) - w_b(t)]\} \quad (24a)$$

$$w_b(t) = F^{-1}\{\exp(-\theta)F[2v_a(t) - w_a(t)]\} \quad (24b)$$

for simulating the propagation delay and the attenuation loss of a lossy transmission line. Equation (24) is the time-domain version of (19) and $\{F, F^{-1}\}$ denote the Fourier and inverse Fourier integrals. Unlike the discrete-time analysis, which requires invoking the FFT routine at every time step, the WR analysis calls for the FFT routine after the completion of each iterative circuit simulation and therefore reduces the overall computer simulation time. The voltage generator waveforms are computed at periodic time intervals $\{t = k\Delta t,\ k = 0,1,2,\cdots,N-1,\ N = 2^p\}$ dictated by the FFT algorithm, whereas terminal voltage waveforms are often computed at nonuniform time intervals since the numerical integration of circuit equations with nonuniform step sizes is more efficient. Thus data interpolation is required. Through linear interpolation the Fourier spectrum of terminal voltage waveforms are computed at integral multiples of the fundamental frequency $f_0(=1/T)$ by finite summation:

$$V(mf_0) = \int_0^T v(t)\exp(-j2\pi mf_0 t)\,dt = \left(\frac{T}{2\pi m}\right)\sum_{k=0}^{2N-1} a_k W_N^{-mk} \quad (25a)$$

$$V(0) = \int_0^T v(t)\,dt = \left(\frac{T}{N}\right)\left\{(1/2)[v(0)+v(T)] + \sum_{k=1}^{N-1} v(kT/N)\right\} \quad (25b)$$

where

$$W_N = \exp(j2\pi/N) \quad (25c)$$

$$a_k = (N/T)[2v(t_k) - v(t_{k-1}) - v(t_{k+1})] \quad (25d)$$

$$v(T) = v(0), \qquad v(t_{-1}) = v(t_{N-1}) \qquad (t_k = kT/N) \quad (25e)$$

and $\{V(f), v(t)\} = \{V_A(f), v_a(t)\}$, $\{V_B(f), v_b(t)\}$ for the near-end and far-end terminal voltages, respectively. Notice that (25e) indicates that periodic, continuous terminal voltage waveforms are constructed from the finite discrete data sets obtained from the circuit simulator. From (25a) we observe that the Fourier spectrum of a linearly interpolated waveform decays in inverse proportion to the square of the frequency if the second derivative (25d) of the waveform is a sufficiently smooth function. Thus it becomes obvious that a higher order polynomial spline [14] can be used to construct a continuous waveform whose Fourier spectrum is almost band-limited so that the spectrum aliasing effect is reduced. Indeed, the Fourier spectrum of a periodic waveform obtained from the cubic spline decays in inverse proportion to the fourth power of the frequency:

$$V(mf_0) = \int_0^T v(t)\exp(-j2\pi mf_0 t)\,dt = 6\left(\frac{T}{2\pi m}\right)^4 \sum_{k=0}^{N-1} b_k W_N^{-mk} \quad (26)$$

where $\{b_k\}$ are obtained by solving a tridiagonal matrix in terms of $\{v(t_i)\}$. Both (25a) and (26) can be numerically computed by applying the FFT [15]:

$$H(m) = \frac{1}{N}\sum_{k=0}^{N-1} h(k) W_N^{-mk} \quad (27a)$$

and the fundamental frequency $(f_0 = 1/T)$ can be made smaller by choosing a time-window size (T) greater than the actual time duration of the terminal voltage waveforms. Reducing f_0 allows more samples of low frequency spectrum to be included in the construction of the voltage generator waveforms (24) using the inverse FFT:

$$h(k) = \sum_{i=0}^{N-1} H(i) W_N^{+ki} \quad (27b)$$

where

$$H(i) = \{\exp[-\theta(f_k)]\,F[2v(t) - w(t)]\}$$

as defined in (24). One should be reminded that the spectrum aliasing effect [15] is reduced by using an almost band-limited spectrum for reconstruction of the time-domain waveforms.

IV. Generalized Method of Characteristics for Waveform Relaxation Analysis of Coupled Lossy Striplines

In Section II we derived the canonical expressions of the lossy coupled stripline terminal voltages. An iteration scheme for generating the infinite series expansion of the canonical solutions defined by (15) has been programmed and implemented in a circuit simulator. We shall describe the computational algorithm first and then the convergence theorem.

The iteration algorithm can be described vividly in terms of the disjoint, symmetrical two-part network of Fig. 5, which is derived from the decoupled equivalent network of Fig. 1 with each of the n decoupled lossy transmission lines replaced by the equivalent disjoint 2-port network of Fig. 3(b). Each part of the two-part network consists of an identical $2n$-terminal congruence transformer whose secondary terminals are connected to the identical set of n decoupled transmission-line characteristic impedances. The

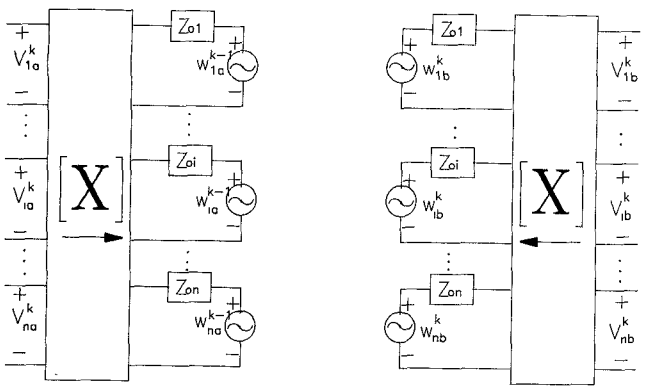

Fig. 5. The equivalent disjoint two-part network of an n-conductor lossy coupled transmission-line system.

congruence transformers are implemented in a circuit simulator with each of the primary terminals connecting to a voltage-dependent voltage source and each of the secondary terminals connecting to a current-dependent current source as defined by (5). The lossy characteristic impedances are synthesized by the ladder network of Fig. 4 with circuit elements $\{R_s = \sqrt{L_i/C_i},\ C_p = 2\sqrt{L_iC_i}/R_i\}$ defined in terms of the decoupled lossy transmission-line parameters. Waveforms generated by the FFT waveform generators $\{w_{ia}^{k-1} w_{ib}^{k},\ i = 1,2,3,\cdots,n\}$ are stored in the $n \times m$ matrices $\boldsymbol{w}_a^{k-1}$ and $\boldsymbol{w}_b^{k}$ with (i, j)th elements designating the voltage amplitudes of the ith pair of generators recorded at $t = t_j$:

$$\left[w_a^{k-1}\right]_{i,j} = w_{ia}^{k-1}(t = t_j)$$

$$\left[w_b^{k}\right]_{i,j} = w_{ib}^{k}(t = t_j) \qquad (1 \leqslant i \leqslant n, 1 \leqslant j \leqslant m)$$

where the superscript k designates the iteration count and the subscripts a and b refer to part (a) and part (b) of the disjoint two-part network. The terminal voltage waveforms at the end of the kth iteration are stored in the $n \times m$ matrices $\boldsymbol{v}_a^k$ and $\boldsymbol{v}_b^k$, with the (i, j)th elements designating the near-end and far-end terminal voltages of the ith conductor at $t = t_j$:

$$\left[\boldsymbol{v}_a^k\right]_{i,j} = v_i^k(x = 0, t = t_j)$$

$$\left[\boldsymbol{v}_b^k\right]_{i,j} = v_i^k(x = l, t = t_j) \qquad (1 \leqslant i \leqslant n, 1 \leqslant j \leqslant m)$$

where the subscripts a and b refer to the near-end and far-end terminals of the stripline system, respectively. The initial terminal voltages and currents are designated by the column vectors $\boldsymbol{v}_{a0}, \boldsymbol{v}_{b0}, \boldsymbol{i}_{a0}, \boldsymbol{i}_{b0}$, which can be derived by performing a dc analysis on the stripline system with each transmission line replaced by a resistor representing the total conductor loss of the transmission line. Exact initial terminal characteristics are reproduced by the two-part network by assigning the FFT waveform generators with the initial values

$$\boldsymbol{w}_{a0} = \boldsymbol{X}^{-1}\boldsymbol{v}_{a0} - \operatorname{diag}\left((2m_i + 1)\sqrt{L_i/C_i}\right)\boldsymbol{X}^t\boldsymbol{i}_{a0}$$

$$\boldsymbol{w}_{b0} = \boldsymbol{X}^{-1}\boldsymbol{v}_{b0} + \operatorname{diag}\left((2m_i + 1)\sqrt{L_i/C_i}\right)\boldsymbol{X}^t\boldsymbol{i}_{b0}.$$

These are derived by replacing each lossy characteristic impedance by the dc driving-point impedance of the equivalent ladder network constructed with m_i sections of symmetrical T networks and assigning the two-part network with the exact terminal characteristics. Refer to Fig. 5: The iteration algorithm is described below.

Combined MC and WR Algorithm (Gauss–Seidel Type)

Step 0: Initialize the iteration counter ($k = 1$) and the FFT waveform generators[4]:

$$\boldsymbol{w}_a^{k-1}[;1] = \boldsymbol{w}_a^{k-1}(t_1 = 0) = \boldsymbol{w}_{a0}$$

$$\boldsymbol{w}_b^{k}[;1] = \boldsymbol{w}_b^{k}(t_1 = 0) = \boldsymbol{w}_{b0}$$

so that the waveform relaxation analysis reproduces exact initial terminal characteristics. Generate the Fourier spectrum of the exponential propagation functions of the n decoupled lossy transmission lines and store the data in the array $[\mathrm{H}]_{i,j} = \exp[-\theta_i(s = s_j)]$.

Step 1: Connect the terminating network A of Fig. 2 to part (a) of the two-part network of Fig. 5 and carry out the transient analysis for the entire time interval ($0 = t_1 \leqslant t \leqslant t_m$) to obtain the near-end terminal voltage waveforms $\{\boldsymbol{v}_a^k(t)\}$. Store the result in the matrix $\boldsymbol{v}_a^k$.

Step 2: Compute $\{\boldsymbol{w}_b^k(t)\}$ from $\{\boldsymbol{v}_a^k(t)\}$ and $\{\boldsymbol{w}_a^{k-1}(t)\}$ by the FFT and the inverse FFT[5] and store the result in the array:

$$\boldsymbol{w}_b^k = \boldsymbol{F}^{-1}\left\{\boldsymbol{H} * \boldsymbol{F}\left[2\boldsymbol{X}^{-1}\boldsymbol{v}_a^k - \boldsymbol{w}_a^{k-1}\right]\right\}.$$

Step 3: Connect the terminating network B of Fig. 2 to the part (b) of the two-part network and carry out the transient analysis for the entire time interval ($0 \leqslant t_1 \leqslant t \leqslant t_m$) to obtain the far-end terminal voltage waveforms $\{\boldsymbol{v}_b^k(t)\}$. Store the result in the matrix $\boldsymbol{v}_b^k$.

Step 4: Update $\boldsymbol{w}_a^k$ in terms of $\{\boldsymbol{v}_b^k(t)\}$ and $\{\boldsymbol{w}_b^k(t)\}$ by the FFT and the inverse FFT:

$$\boldsymbol{w}_a^k = \boldsymbol{F}^{-1}\left\{\boldsymbol{H} * \boldsymbol{F}\left[2\boldsymbol{X}^{-1}\boldsymbol{v}_b^k - \boldsymbol{w}_b^k\right]\right\}.$$

Step 5: Stop the iteration if the iteration count exceeds a preset integral number or if the difference between the results obtained in successive iterations is sufficiently small. Otherwise, set $k = k + 1$ and go to step 1 to repeat the iteration process.

Convergence Theorem of the Combined MC and WR Algorithm (Gauss–Seidel Type): For an n-conductor lossy stripline system terminating in the Thevenin's equivalent circuits of Fig. 2, the combined MC and WR algorithm generates a sequence of waveforms $\{\boldsymbol{v}_a^k(t)\}, \{\boldsymbol{v}_b^k(t)\}$ converging to the exact solution of the terminal voltages given by (11).

Proof: The theorem will be verified in terms of frequency-domain parameters. Refer to Figs. 2 and 5. The kth iteration step of the MC and WR algorithm is transformed into the following system of matrix difference

[4] $\boldsymbol{A}[i;]$ and $\boldsymbol{A}[;j]$ designate the ith row and jth column of the $\boldsymbol{A}$ matrix, respectively.

[5] Term-by-term product of two matrices $\boldsymbol{A}$ and $\boldsymbol{B}$ of identical order is defined as $\boldsymbol{C} = \boldsymbol{A} * \boldsymbol{B}$ with $[\boldsymbol{C}]_{i,j} = [\boldsymbol{A}]_{i,j} \times [\boldsymbol{B}]_{i,j}$.

equations:

$$\boldsymbol{V}_A^k(s) = (1/2)\left[(\boldsymbol{I}_n - \rho_A)\boldsymbol{E}_A + (\boldsymbol{I}_n + \rho_A)\boldsymbol{X}\boldsymbol{W}_A^{k-1}(s)\right] \tag{28a}$$

$$\boldsymbol{X}\boldsymbol{W}_B^k(s) = \boldsymbol{\Phi}\left[2\boldsymbol{V}_A^k(s) - \boldsymbol{X}\boldsymbol{W}_A^{k-1}(s)\right] \tag{28b}$$

$$\boldsymbol{V}_B^k(s) = (1/2)\left[(\boldsymbol{I}_n - \rho_B)\boldsymbol{E}_B + (\boldsymbol{I}_n + \rho_B)\boldsymbol{X}\boldsymbol{W}_B^{k-1}(s)\right] \tag{28c}$$

$$\boldsymbol{X}\boldsymbol{W}_A^k(s) = \boldsymbol{\Phi}\left[2\boldsymbol{V}_B^k(s) - \boldsymbol{X}\boldsymbol{W}_B^k(s)\right] \tag{28d}$$

where $\boldsymbol{\Phi}$ and $\{\rho_A, \rho_B\}$ are defined in (9d) and (14). Equation (28) can be solved by successive elimination of variables, leading to the solution

$$\boldsymbol{V}_A^{k+1} = \boldsymbol{U}_A + \boldsymbol{P}\boldsymbol{V}_A^k(s) \tag{29a}$$

$$\boldsymbol{V}_B^{k+1} = \boldsymbol{U}_B + \boldsymbol{Q}\boldsymbol{V}_B^k(s) \tag{29b}$$

where $\{\boldsymbol{P}, \boldsymbol{Q}\}$ and $\{\boldsymbol{U}_A, \boldsymbol{U}_B\}$ are identified as the propagation matrices and the equivalent voltage sources defined in (12) and (13). From (28a), we obtain

$$\boldsymbol{V}_A^1(s) = (1/2)\left[(\boldsymbol{I}_n - \rho_A)\boldsymbol{E}_A + (\boldsymbol{I}_n + \rho_A)\boldsymbol{X}(1/s)\boldsymbol{w}_{a0}\right]$$

where $(1/s)\boldsymbol{w}_{a0}$ is the vector step function generating the correct initial near-end terminal characteristics of the stripline system as described in step 0 of the MC and WR algorithm. Thus by carrying out repeated substitutions into (29a), we obtain the following sequence of waveforms:

$$\begin{aligned}
\boldsymbol{V}_A^2(s) &= \boldsymbol{U}_A + \boldsymbol{P}\boldsymbol{V}_A^1(s)\\
\boldsymbol{V}_A^3(s) &= (\boldsymbol{I}_n + \boldsymbol{P})\boldsymbol{U}_A + \boldsymbol{P}^2\boldsymbol{V}_A^1(s)\\
\boldsymbol{V}_A^4(s) &= (\boldsymbol{I}_n + \boldsymbol{P} + \boldsymbol{P}^2)\boldsymbol{U}_A + \boldsymbol{P}^3\boldsymbol{V}_A^1(s)\\
&\cdots\cdots\cdots\cdots\cdots\cdots\cdots\cdots\cdots\cdots\\
\boldsymbol{V}_A^k(s) &= (\boldsymbol{I}_n + \boldsymbol{P} + \boldsymbol{P}^2 + \cdots + \boldsymbol{P}^{k-2})\boldsymbol{U}_A + \boldsymbol{P}^{k-1}\boldsymbol{V}_A^1(s)\\
&= (\boldsymbol{I}_n - \boldsymbol{P}^{k-1})(\boldsymbol{I}_n - \boldsymbol{P})^{-1}\boldsymbol{U}_A + \boldsymbol{P}^{k-1}\boldsymbol{V}_A^1(s)
\end{aligned}$$

which is identical to (15a) except for the residue term $\boldsymbol{P}^{k-1}\boldsymbol{V}_A^1(s)$ related to the initial condition of the stripline system. Similarly, we obtain

$$\boldsymbol{V}_B^k(s) = (\boldsymbol{I}_n - \boldsymbol{Q}^{k-1})(\boldsymbol{I}_n - \boldsymbol{Q})^{-1}\boldsymbol{U}_B + \boldsymbol{Q}^{k-1}\boldsymbol{V}_B^1(s)$$

which is identical to (15b) except for the residue term $\boldsymbol{Q}^{k-1}\boldsymbol{V}_B^1(s)$. For k approaching infinity, the residue terms vanish if the eigenvalues of the propagation matrices $(\boldsymbol{P}, \boldsymbol{Q})$ are confined in the left half of the s plane, which is usually the case for a stable system. This completes the proof of the theorem.

In the next section, a three-conductor lossy directional coupler driven by a bipolar ECL gate is simulated to illustrate the advantage of the waveform relaxation over the classical discrete-time simulation.

V. Waveform Relaxation Analysis of a Lossy Directional Coupler

Let us start this section by stating an important directional coupler theory. The proof and the experimental verification of the theory can be found in [17].

Distortionless Signal Transmission Theory: In a triconductor lossless transmission-line system of length l, wave propagation velocity v, and PUL transmission-line parameters $\{L_{ij}\}$ and $\{C_{ij}\}$, each signal generator $\{e_i(t),\ i = 1,2,3\}$ applied to a sending terminal $(x = 0)$ will produce at the corresponding far-end terminal $(x = l)$ an output with the identical generator waveshape if the internal resistors $\{r_{ia}\}$ of the generators and the load resistors $\{r_{ib}\}$ are adjusted to the values

$$\begin{aligned}
\boldsymbol{Z}_A &= \operatorname{diag}(r_{1a}, r_{2a}, r_{3a})\\
&= r_{1a}\operatorname{diag}\left[1, (L_{23}C_{13}/C_{23}L_{13}), (L_{23}C_{12}/C_{23}L_{12})\right]
\end{aligned} \tag{30a}$$

$$\begin{aligned}
\boldsymbol{Z}_B &= \operatorname{diag}(r_{1b}, r_{2b}, r_{3b})\\
&= (L_{12}L_{13}C_{23}/C_{12}C_{13}L_{23})(1/r_{1a})^2\boldsymbol{Z}_A
\end{aligned} \tag{30b}$$

where r_{1a} is defined by the quadratic equation

$$r_{1a}^2 + a_1 r_{1a} + a_0 = 0 \tag{30c}$$

with parameters

$$a_0 = (L_{12}/C_{12})(L_{13}/C_{13})(C_{23}/L_{23}) \tag{30d}$$

$$a_1 = -vL_{11}\left[1 + a_0(C_{11}/L_{11})\right]. \tag{30e}$$

Under such a terminating condition, the receiving signals across the load resistors are delayed and attenuated by the same magnitudes:

$$v_i(t, l) = -(a_0/a_1 r_{1a})e_i(t - l/v) \qquad (i = 1,2,3). \tag{31}$$

In the following example we shall examine the effect of the conductor loss on such a distortionless signal transmission property of a triconductor directional coupler.

Consider a triconductor stripline system of length $l = 10\sqrt{2}$ cm, wave propagation velocity $v = \sqrt{2}\cdot 10^{10}$ cm/s, and transmission-line parameters

$$\boldsymbol{L} = \begin{bmatrix} 3 & 1 & 0.5 \\ 1 & 4 & 1 \\ 0.5 & 1 & 3 \end{bmatrix} \text{nH/cm}$$

$$\boldsymbol{C} = (1/24)\begin{bmatrix} 44 & -10 & -4 \\ -10 & 35 & -10 \\ -4 & -10 & 44 \end{bmatrix} \text{pF/cm}.$$

The center conductor and the active outer conductor are connected to the in-phase and the out-of-phase outputs of a bipolar ECL gate as shown in Fig. 6. The inactive outer conductor is connected to ground via r_{3a}.

Case 1 — Lossless Conductors: $\boldsymbol{R} = \operatorname{diag}(0, 0, 0)$

From (30) we obtain the terminating resistors

$$\boldsymbol{Z}_A = 5\sqrt{2}\operatorname{diag}(5,4,5) \qquad \boldsymbol{Z}_B = 12\sqrt{2}\operatorname{diag}(5,4,5)\ \Omega \tag{32a}$$

for distortionless signal transmission. The ECL gate output signals arrive at the far-end terminals with 1 ns delay and are attenuated by a factor of 17/12:

$$v_i(t, l) = (12/17)e_i(t - 1)u(t - 1) \qquad (i = 1,2). \tag{32b}$$

The distortionless signal transmission property can also be verified from (11b). Thus substituting $\boldsymbol{Z}_A, \boldsymbol{Z}_B$ and $\boldsymbol{Z}_0 = v\boldsymbol{L}$

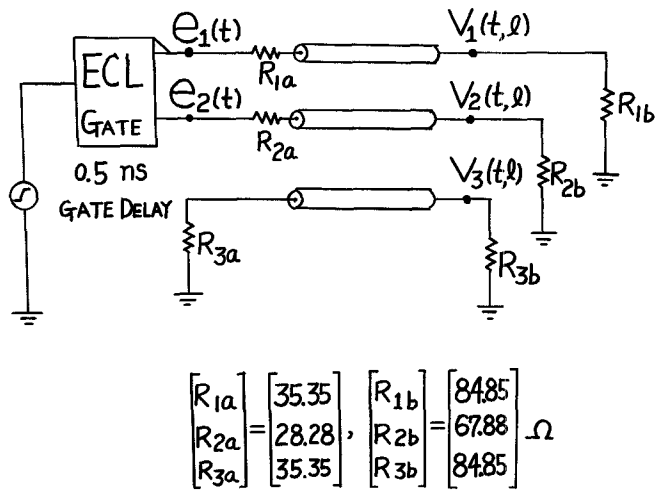

$$\begin{bmatrix} R_{1a} \\ R_{2a} \\ R_{3a} \end{bmatrix} = \begin{bmatrix} 35.35 \\ 28.28 \\ 35.35 \end{bmatrix}, \quad \begin{bmatrix} R_{1b} \\ R_{2b} \\ R_{3b} \end{bmatrix} = \begin{bmatrix} 84.85 \\ 67.88 \\ 84.85 \end{bmatrix} \Omega$$

Fig. 6. A three-conductor lossy directional coupler driven by a bipolar ECL gate.

into (14), we obtain the reflection matrices:

$$\rho_A = -(1/34)\begin{bmatrix} 2 & 5 & 2 \\ 4 & 10 & 4 \\ 2 & 5 & 2 \end{bmatrix}$$

$$\rho_B = (1/34)\begin{bmatrix} 12 & -5 & -2 \\ -4 & 4 & -4 \\ -2 & -5 & 12 \end{bmatrix}$$

which reveal the orthogonal property of the reflection matrices $\rho_A \rho_B = 0$. Equation (11b) degenerates into the simple form

$$V(l) = (12/17)\exp(-s\tau)E_A(s), \qquad \tau = 1 \text{ ns}$$

which is the Laplace transform of (32b).

Case 2 — Lossy Conductors: $\boldsymbol{R} = \text{diag}(2, 4, 2)\ \Omega/cm$

To obtain the equivalent decoupled circuit (Fig. 1) and the two-part disjoint network (Fig. 5) for analyzing the transient response of the lossy stripline system, we proceed as follows.

Step 1: By using the Jacobi method [16], we diagonalize the time-constant matrix:

$$\boldsymbol{T} = \boldsymbol{R}^{-1/2}\boldsymbol{L}\boldsymbol{R}^{-1/2} = (1/4)\begin{bmatrix} 6 & \sqrt{2} & 1 \\ \sqrt{2} & 4 & \sqrt{2} \\ 1 & \sqrt{2} & 6 \end{bmatrix}$$

$$= \boldsymbol{W}\,\text{diag}(\tau_1, \tau_2, \tau_3)\boldsymbol{W}^{-1}$$

$$\boldsymbol{W} = (1/\sqrt{10})\begin{bmatrix} 1 & \sqrt{5} & 2 \\ -2\sqrt{2} & 0 & \sqrt{2} \\ 1 & -\sqrt{5} & 2 \end{bmatrix},$$

$$\boldsymbol{W}^{-1} = \boldsymbol{W}^t, \quad \tau_1, \tau_2, \tau_3 = (3/4, 5/4, 2) \text{ ns}.$$

Step 2: Let $(L_1, L_2, L_3) = (5/3, 5, 5/2)$ nH/cm and obtain the congruence transformer matrix:

$$\boldsymbol{X} = \boldsymbol{R}^{1/2}\boldsymbol{W}\,\text{diag}\left(\sqrt{\tau_1/L_1}, \sqrt{\tau_2/L_2}, \sqrt{\tau_3/L_3}\right)$$

$$= (1/10)\begin{bmatrix} 3 & 5 & 8 \\ -12 & 0 & 8 \\ 3 & -5 & 8 \end{bmatrix}.$$

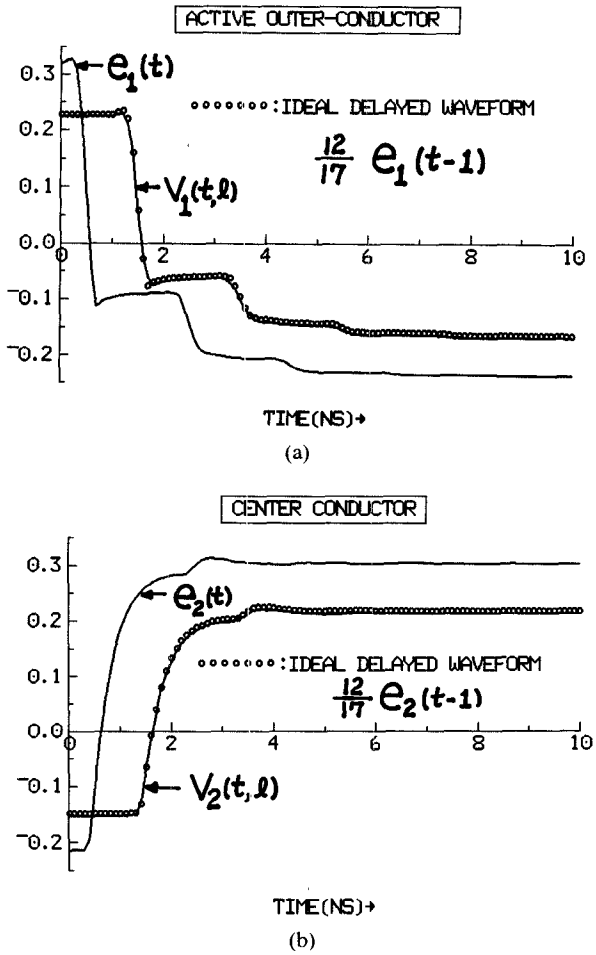

Fig. 7. Distortionless signal transmission in a lossless triconductor system. (a) ECL gate out-of-phase output and its delayed waveform. (b) ECL gate in-phase output and its delayed waveform.

Step 3: Obtain from (7) the decoupled transmission-line parameters:

$$(L_1, L_2, L_3) = (5/3, 5, 5/2) \text{ nH/cm}$$

$$(C_1, C_2, C_3) = (3, 1, 2) \text{ pF/cm}$$

$$(R_1, R_2, R_3) = (20/9, 4, 5/4)\ \Omega/\text{cm}.$$

Step 4: Obtain from (22) the circuit parameters:

$$(R_{1s}, R_{2s}, R_{3s}) = (23.57, 70.71, 35.35)\ \Omega$$

$$(C_{1p}, C_{2p}, C_{3p}) = (63.64, 35.35, 113.14) \text{ pF}$$

of the symmetrical T networks for the Padé synthesis of the characteristic impedances of the decoupled lossy transmission lines.

Step 5: Derive the propagation functions of the decoupled lines:

$$\left\{\theta_i(s) = (sl/v)\sqrt{1 + (1/s\tau_i)}\right\}$$

$$= \tilde{s}\left(\sqrt{1 + 4/3\tilde{s}}, \sqrt{1 + 4/5\tilde{s}}, \sqrt{1 + 1/2\tilde{s}}\right)$$

where $\tilde{s}$ = normalized angular frequency $= 10^{-9}\, j\omega$.

Shown in Figs. 7 and 8 are the ECL gate outputs and the receiving-end waveforms simulated with and without the conductor loss. The distortionless transmission prop-

erty is evident in the lossless system and is remarkably preserved even in the presence of the conductor loss. The lossless system is simulated by the classical MC, which takes up 15.19 seconds of computer simulation time and uses 273 kbytes of memory, which includes 156 kbytes for loading the circuit simulator (ICD) into the IBM 3090 computer. The penalty of using the classical MC for analyzing the lossy stripline system is severe. It took 635 seconds of CPU time and used up 2 megabytes of computer memory. The waveforms in Fig. 8 are obtained by discrete-time simulation with very small time steps, and 40 sections of lossless lines cascaded with lumped resistors are used for simulating the distributed nature of the conductor loss. Waveforms obtained from the iterative relaxation analyses are shown in Fig. 9. The waveform relaxation analyses consumed 22.1 seconds and used 233 kbytes of memory. From the simulated waveforms, we observe that two iterations are sufficient to obtain the convergent solutions. To estimate the accuracy of the waveform relaxation analysis, it is assumed that the waveform $v(t)$ obtained from the discrete-time analysis with very small time steps (shown in Fig. 8) is exact, and the average absolute difference between the waveforms obtained by relaxation and discrete-time analyses:

$$\delta = \left[\int_0^T |\tilde{v}(t) - v(t)|\, dt\right] \Big/ T$$

is defined as the absolute error of the waveform $\tilde{v}(t)$ obtained from WR analysis. It is observed that the accuracy of the GMC can be enhanced by lowering the fundamental frequency ($f_0 = 1/T', T' > T$) of spectrum sampling so that more samples of low frequency spectra are included in the construction of the time-domain waveforms.

Table I presents the absolute errors of the (center-conductor) receiving-end waveforms generated by the GMC using various FFT samples and time-window enlargement factors (T'/T). Observe that enlarging the time-window size for improving the accuracy of FFT would work only if the number of sampled data points used in the FFT were no less than $N = 256$. We use the directional coupler as an example to demonstrate the accuracy of the waveform relaxation method. As shown in Fig 9, the receiving signal at the far end of the inactive outer conductor has a peak amplitude 10 times smaller than that observed at the two ends of the center conductor. Here, the mean absolute difference between the waveform relaxation and discrete-time analyses is measured in tenths of millivolts. The extreme accuracy of the waveform relaxation is achieved by reducing the spectrum aliasing effect in the FFT by using nearly band-limited interpolated waveforms.

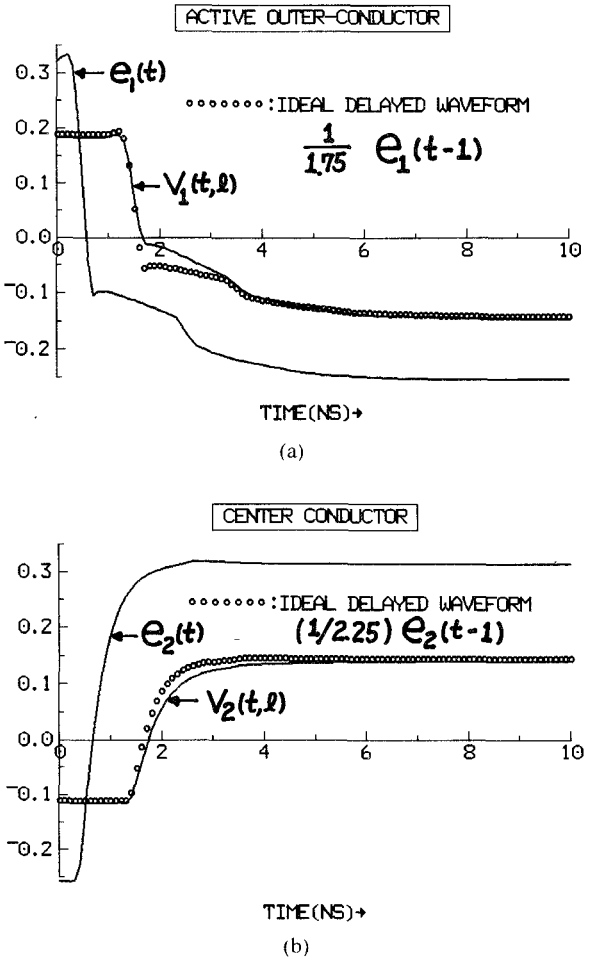

Fig. 8. Almost distortionless signal transmission in a lossy triconductor system. (a) ECL gate out-of-phase output and its delayed waveform. (b) ECL gate in-phase output and its delayed waveform.

VI. Conclusions

An efficient method for computing the transient response of an n-conductor lossy coupled transmission line system is presented. The method consists in performing waveform relaxation analysis on the equivalent two-part disjoint network of the coupled-line system derived from the congruence transformation theory and the method of characteristics. The Padé synthesis of the irrational lossy characteristic impedance function and the fast Fourier transform for simulating the wave propagation delay and attenuation have been utilized to enhance the method of characteristics for the analysis of coupled distributed networks. Although the method of characteristics dates back to the 1747 classic work of D'Alembert, it was not until Branin's pioneering work on the analysis of an ideal transmission line that it was transformed into an indispensable tool for the computer-aided analysis of coupled distributed networks. Here, we have opened up yet another horizon by generalizing the method of characteristics for the waveform relaxation analysis. In separate articles, we shall explore many other applications of the generalized method of characteristics, which include waveform relaxation analyses of the diode switching characteristics [18], an RLCG transmission line [13], VLSI circuits interconnected with coupled transmission lines [19], and nonuniform transmission lines [20].

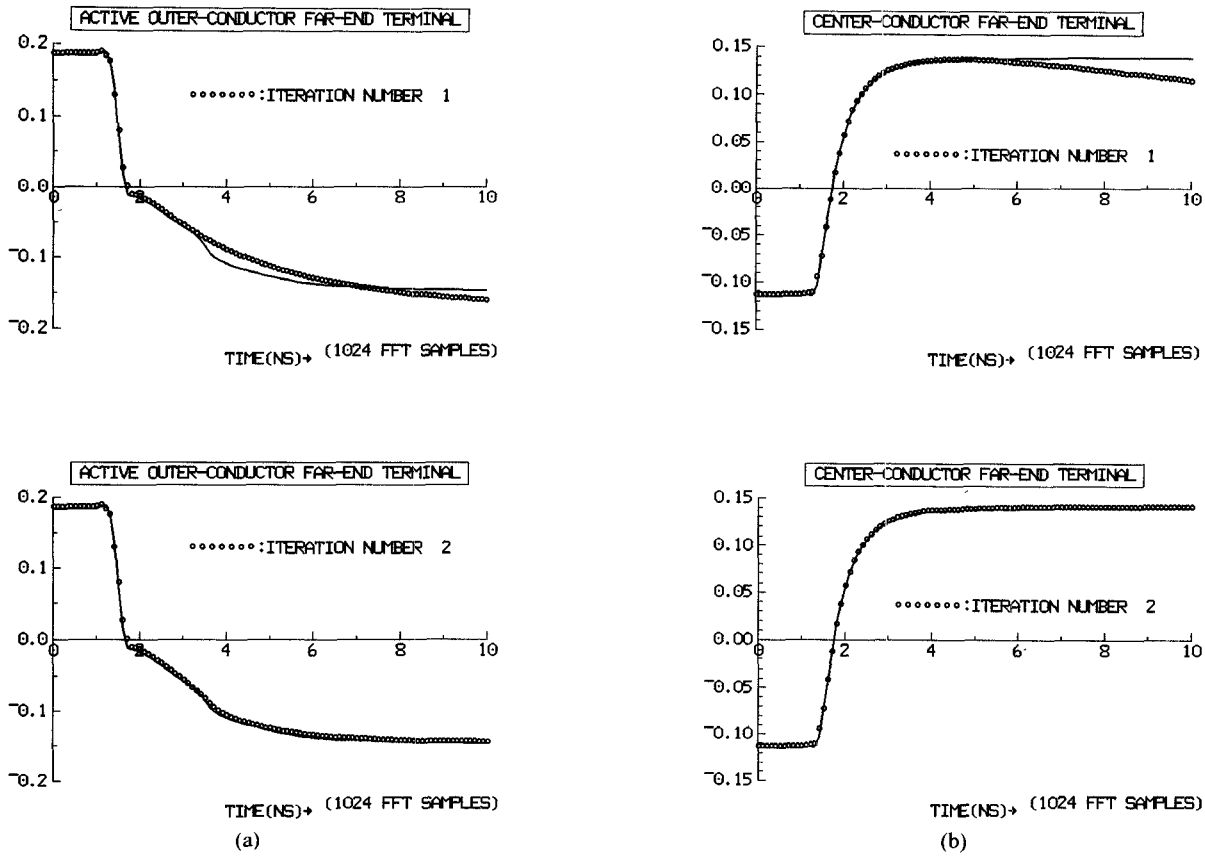

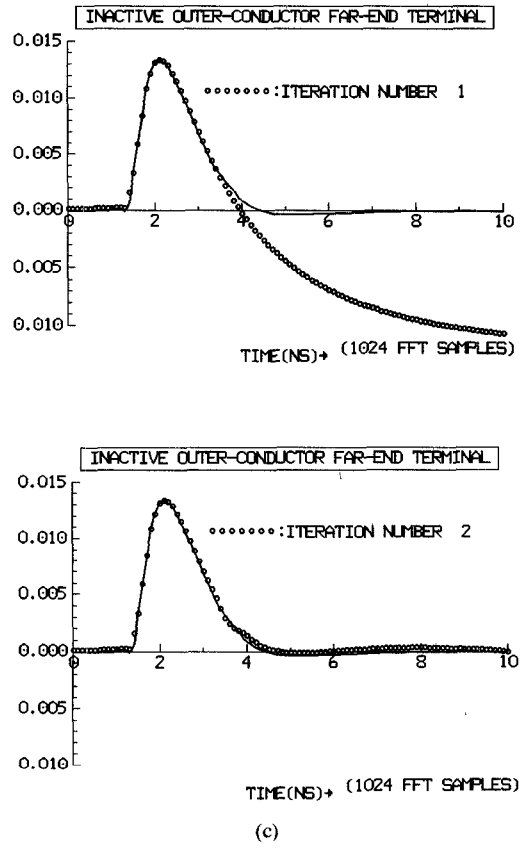

Fig. 9. Waveforms generated by the iterated waveform relaxation analyses. Waveforms at the far-end terminal of the (a) active outer conductor, (b) center conductor, and (c) inactive outer conductor.

TABLE I

N	δ : absolute error(mv) T'/T=2	T'/T=4	T'/T=8	% cpu FFT
32	14.00	9.00	23.82	0.45
64	10.65	5.95	7.82	0.63
128	10.09	2.51	4.82	0.81
256	9.91	1.99	1.37	1.53
512	9.85	1.75	0.86	2.80
1024	9.82	1.72	0.61	4.97

ACKNOWLEDGMENT

The author wishes to thank his students P. Saviz and W. Beyene of Columbia University for proofreading the manuscript and providing the drawings.

REFERENCES

[1] M. Lister, "The numerical solution of hyperbolic partial differential equations by the method of characteristics," in *Mathematical Methods for Digital Computer*, A. Ralston and H. S. Wilf, Eds. New York: Wiley, 1960, ch. 15.

[2] E. Lelarasmee, A. E. Ruehli, and A. L. Sangiovanni-Vincentelli, "The waveform relaxation method for time-domain analysis of large scale integrated circuits," *IEEE Trans. Computer-Aided Design*, vol. CAD-1, pp. 131–145, July 1982.

[3] F. H. Branin, Jr., "Transient analysis of lossless transmission line," *Proc. IEEE*, vol. 55, pp. 2012–2013, Nov. 1967.

[4] F. Y. Chang, "Transient analysis of lossless coupled transmission lines in a nonhomogeneous dielectric medium," *IEEE Trans. Microwave Theory Tech.*, vol. MTT-18, pp. 616–626, Sept. 1970.

[5] R. Courant and K. O. Friedrichs, *Supersonic Flow and Shock Waves*. New York: Interscience, 1948.

[6] C. W. Ho, "Theory and computer-aided analysis of lossless transmission lines," *IBM J. Res. Develop.*, vol. 17, pp. 249–255, 1973.

[7] K. D. Marx, "Propagation modes, equivalent circuits, and characteristic terminations for multiconductor transmission lines with inhomogeneous dielectric," *IEEE Trans. Microwave Theory Tech.*, vol. MTT-21, pp. 450–457, July 1973.

[8] F. Y. Chang, "Computer-aided characterization of coupled TEM transmission lines," *IEEE Trans. Circuits Syst.*, vol. CAS-27, pp. 1194–1205, Dec. 1980.

[9] J. White and A. L. Sangiovanni-Vincentelli, "RELAX2: A new waveform relaxation approach for the analysis of LSI MOS circuits," in *Proc. 1983 Int. Symp. Circuits Syst.*, May 1983.

[10] A. R. Newton and A. L. Sangiovanni-Vincentelli, "Relaxation-based electrical simulation," *IEEE Trans. Computer-Aided Design*, vol. CAD-3, pp. 308–330, Oct. 1984.

[11] *Interactive Circuit Design User's Guide*, IBM Corp., Data Proc. Div., White Plains, N.Y., pub. no. SH20-2336-0.

[12] H. S. Wall, *Analytic Theory of Continued Fraction*. Princeton, NJ: D. Van Nostrand, 1984, ch. 20., sec. 95.

[13] F. Y. Chang, "The generalized method of characteristics for waveform relaxation analysis of an RLCG transmission line," to be submitted for publication.

[14] J. Ahlberg, E. Nilson, and J. Walsh, *The Theory of Splines and Their Applications*. New York: Academic Press, 1967.

[15] E. O. Brigham, *The Fast Fourier Transform*. Englewood Cliffs, NJ: Prentice Hall, 1974.

[16] A. Ralston and H. S. Wilf, *Mathematical Methods for Digital Computers*. New York: Wiley, 1960, pp. 84–91.

[17] F. Y. Chang, "Multiconductor, arbitrary geometry, directional coupler theory," IBM Tech. Rep. TR22.865, Component Division, East Fishkill, Oct. 10, 1969.

[18] F. Y. Chang, "Waveform relaxation analysis of diode switching characteristics," to be submitted for publication.

[19] F. Y. Chang, "Waveform relaxation analysis of VLSI interconnected with coupled transmission lines," to be submitted for publication.

[20] F. Y. Chang, "Waveform relaxation analysis of nonuniform lossy coupled transmission lines," in preparation.

✠

Fung-Yuel Chang (M'68–SM'88) received the B.S. degree in electrical engineering from National Cheng Kung University, Taiwan, China, in 1959, the M.S. degree in electronics from the National Chiao Tung University, Taiwan, in 1961, and the M.S. and Eng.Sc.D degrees, both in electrical engineering, from Columbia University, New York, NY, in 1964 and 1968, respectively.

He has been with the IBM General Technology Division in East Fishkill, NY, since 1968. His first job assignment at IBM led to pioneering work on the method of characteristics for transient simulation of integrated circuits interconnected with multiconductor coupled transmission lines. He received the IBM corporate outstanding innovation award for his design and modeling of bipolar transistors implemented in three generations of IBM mainframe computers. In 1984, he was a Visiting Associate Professor of Electrical Engineering at Columbia University, where he taught courses on bipolar device modeling and computer-aided circuit analysis. Prior to his sabbatical leave from IBM, he was a senior engineering manager of the Bipolar Device Design and Modeling Department. Since 1985, he has been an adjunct professor at Columbia University. At IBM, he is presently engaged in applying waveform relaxation techniques to packaging analysis. His areas of interest include distributed network theory, device modeling, computer-aided circuit analysis, and VLSI interconnection theory.